

**Characterization of  
MIPAS elevation  
pointing**

M. Kiefer et al.

# Characterization of MIPAS elevation pointing

**M. Kiefer<sup>1</sup>, T. von Clarmann<sup>1</sup>, U. Grabowski<sup>1</sup>, M. De Laurentis<sup>2</sup>, R. Mantovani<sup>3</sup>,  
M. Milz<sup>1</sup>, and M. Ridolfi<sup>4</sup>**

<sup>1</sup>Forschungszentrum Karlsruhe, Institut für Meteorologie und Klimaforschung, Karlsruhe, Germany

<sup>2</sup>Operational MIPAS mission planner for ESA, Rhea System SA, Louvain-La-Neuve, Belgium

<sup>3</sup>Responsible for operational MIPAS mission calibration for ESA from 2002 to 2005 – Vitrociset S.p.A., Rome, Italy

<sup>4</sup>Dip.to di Chimica Fisica e Inorganica, Università di Bologna, Italy

Received: 24 October 2006 – Accepted: 7 December 2006 – Published: 13 December 2006

Correspondence to: M. Kiefer (michael.kiefer@imk.fzk.de)

Title Page

Abstract

Introduction

Conclusions

References

Tables

Figures

◀

▶

◀

▶

Back

Close

Full Screen / Esc

Printer-friendly Version

Interactive Discussion

Abstract

Sufficient knowledge of the pointing is essential for analyses of limb emission measurements. The scientific retrieval processor for MIPAS operated at IMK allows to retrieve pointing information in terms of tangent altitudes along with temperature. The retrieved tangent altitudes are independent of the engineering Line-Of-Sight (LOS) information delivered with the ESA Level 1b product. The difference of pointing retrieved from the reprocessed high resolution MIPAS spectra and the engineering pointing information was examined with respect to spatial/temporal behaviour. Among others the following characteristics of MIPAS pointing could be identified: Generally the engineering tangent altitudes are too high by 0–1.8 km with conspicuous variations in this range over time. Prior to December of 2003 there was a drift of about 50–100 m/h, which was due to a slow change in the satellite attitude. A correction of this attitude is done twice a day, which led to discontinuities in the order of up to 2 km in the tangent altitudes. There is a systematic difference in the mispointing between the poles which amounts to 1.5–2 km, i.e. there is a conspicuous orbit-periodic feature. The analysis of the correlation between the instrument's viewing angle azimuth and differential mispointing supports the hypotheses that a major part of this latter phenomenon can be attributed to an uncorrected roll angle of the satellite/instrument system of approximately 54 mdeg. Complementary to this, ESA operational LOS calibration results were used to characterize MIPAS pointing. For this purpose MIPAS is used as a radiometer while the passage of infrared bright stars through the instrument's field of view is recorded. Deviation from expected time of passage gives information about mispointing. A pronounced seasonal variation of the LOS is seen before a correction of on-board software took place in December of 2003. Further a pitch bias of 24 mdeg with respect to the platform attitude information is found.

Characterization of MIPAS elevation pointing

M. Kiefer et al.

Title Page

Abstract

Introduction

Conclusions

References

Tables

Figures

◀

▶

◀

▶

Back

Close

Full Screen / Esc

Printer-friendly Version

Interactive Discussion

# 1 Introduction

## 1.1 Motivation

Retrieval of atmospheric state variables from limb emission measurements such as MIPAS (Fischer and Oelhaf, 1996) requires the inverse solution of the radiative transfer equation for the given observation geometry. Obviously, any error in the assumptions on the observation geometry, in particular the tangent altitudes, map directly onto the retrieved state variables. In order not to have to rely completely on Envisat space craft position and attitude and MIPAS scan mirror position information, methods have been developed to retrieve tangent altitude information directly from the spectra, either in terms of tangent point pressure (Ridolfi et al., 2000), or in terms of geometrical tangent altitudes (von Clarmann et al., 2003). While the characterization of the observation geometry by adjusting tangent altitude pressures sufficiently avoids the propagation of tangent altitude errors to retrieved state variables, the retrieval of the tangent altitudes supports more convenient direct comparison to the tangent altitudes inferred from spacecraft position and attitude and scan mirror position information. Any independent characterization of the orbit and attitude parameters is not only relevant to the MIPAS instrument but also to the other limb-viewing instruments onboard Envisat, GOMOS (Kyrölä et al., 2004; Bertaux et al., 2004) and SCIAMACHY (Bovensmann et al., 1999).

## 1.2 MIPAS setup

MIPAS has been designed to operate in either of two pointing regimes: rearward in the Envisat anti-flight direction and sideways in the anti-sun side of the satellite, as illustrated in Fig. 1. The azimuth and elevation angles,  $\alpha$  and  $\epsilon$  respectively, (see Fig. 1) of the Instantaneous Field-Of-View (IFOV) can move within a maximum allowed range called Extended Field-Of-View (EFOV) defined as follows: the azimuth angle can vary from  $74.30^\circ$  to  $110.55^\circ$  in the rearward direction and from  $159.05^\circ$  to  $190.56^\circ$

### Characterization of MIPAS elevation pointing

M. Kiefer et al.

Title Page

Abstract

Introduction

Conclusions

References

Tables

Figures

◀

▶

◀

▶

Back

Close

Full Screen / Esc

Printer-friendly Version

Interactive Discussion

in the sideways direction, the elevation angle can vary from  $113.06^\circ$  to  $117.50^\circ$  in both directions.

Due to this setup, MIPAS pointing is particularly sensitive to the orientation of the satellite x- and y-axes (as illustrated in Fig. 1). The instrument, therefore, can be exploited to determine accurate estimates of pitch and roll angles respectively. This can be done in different ways. In this paper we shall present results from two methods. First there is the operational Line-Of-Sight (LOS) calibration by dedicated measurements as performed by ESA. This method and the corresponding results will be described in detail in Sect. 4. Secondly there is the approach to infer the tangent altitude from a combined temperature/LOS retrieval.

### 1.3 Retrieval method

MIPAS tangent altitude pointing information is retrieved along with the actual temperature profile from  $\text{CO}_2$  spectral lines.  $\text{CO}_2$  is an appropriate tracer for the air mass along the line of sight, since its mixing ratio is sufficiently constant with altitude, and its infrared emissions are, contrary to those of  $\text{O}_2$  or  $\text{N}_2$ , whose altitude distributions are even better predictable, strong enough for an accurate retrieval. The selection of  $\text{CO}_2$  transitions, regularization, and numerical representation of retrieved quantities are discussed in detail in von Clarmann et al. (2003), along with a detailed error budget. In table 4 of the latter paper there are presented estimates of the total error of retrieved tangent altitudes: 260 m below 15 km altitude, less than 200 m from 15 km to 21 km, 150 m or less from 21 km to 27 km, and then less than 200 m up to 68 km.

### 1.4 Scope of this work

In Sects. 2–3 we take the engineering tangent altitudes as delivered with the ESA data products as a reference to define mispointing. In Sect. 4 the absolute pointing knowledge is addressed. The engineering tangent altitudes, at the time of the data processing, represent the best knowledge of the tangent altitudes available from inputs

## Characterization of MIPAS elevation pointing

M. Kiefer et al.

Title Page

Abstract

Introduction

Conclusions

References

Tables

Figures

◀

▶

◀

▶

Back

Close

Full Screen / Esc

Printer-friendly Version

Interactive Discussion

partly measured and partly modelled: satellite position and attitude, scan mirror attitude, Earth shape, and atmospheric refraction. It is delivered together with the Level 1b (L1b) and Level 2 (L2) products. L2 products additionally come with a corrected altitude. This is calculated by building up an hydrostatic atmosphere from the retrieved pressure and temperature values, anchored at the lowest engineering tangent altitude (Ridolfi et al., 2000). Clearly the quality of this corrected altitude critically depends on the accuracy of the engineering tangent altitude of the lowest tangent point.

The majority of MIPAS data was taken in a measurement mode such that the line of sight (LOS) is essentially backwards with respect to the satellite flight direction (see Fig. 1). In this paper we solely consider data of this backward looking mode. To implement a Sun-synchronous orbit the orbital plane is inclined such that the North Pole is on the right side of the flight path (with respect to flight direction), while the South Pole is on its left side. The LOS azimuth  $\alpha$  is changed over the orbit from exactly backwards ( $=90^\circ$ ) to enhance the coverage of regions beyond the latitude turning points of the orbit. There it is driven up to  $110^\circ$  in the vicinity of the North Pole while near the South Pole it reaches down to  $75^\circ$ . Between these two extremes there are several discontinuous changes with small steps near the poles and increasingly bigger steps from middle to equatorial latitudes.

In Sects. 2–3 we consider reprocessed data from mid 2002 to 26 March 2004. This is the time range between the first orbit series which covers entire days and the failure of MIPAS’s scan mirror mechanism on 26 March 2004. This time period includes 12 December 2003, which corresponds to orbit 9321, the date of the update of the PSO (French acronym for on-orbit position) software. The update was necessary because there was an error in the PSO software leading to a periodic change of the satellite attitude with a period of one year.

Characterization of  
MIPAS elevation  
pointing

M. Kiefer et al.

Title Page

Abstract

Introduction

Conclusions

References

Tables

Figures

◀

▶

◀

▶

Back

Close

Full Screen / Esc

Printer-friendly Version

Interactive Discussion

## 2 Altitude dependence

We take as reference the engineering tangent altitude (ETA)  $h_{\text{ETA},i}, i=1 \dots 17$  as delivered with the L1b product of ESA. The altitude grid is roughly defined as  $h_{\text{ETA},i} = 6(3)42(5)52(8)68 \text{ km}$ , but the lowest tangent altitude, as well as the spacing, is slightly modified over the orbit. The altitudes set  $h_{\text{IMK},i}, i=n_{\text{low}} \dots 17$  given by the IMK LOS retrieval results may not always have  $n_{\text{low}}=1$ , i.e. 17 values because spectra of low heights with features caused by cloud emission, are removed prior to retrieval. Therefore we will not be able to assess  $h_{\text{ETA},i}$  for all altitudes always. At the  $i$ th tangent altitude we examine the difference  $\Delta h_i = h_{\text{IMK},i} - h_{\text{ETA},i}$ . A value of  $\Delta h_i$  greater than zero means that the retrieved tangent altitude is larger than the ETA, i.e. the ETA value delivered with the ESA data product gives too low an altitude. In other words  $\Delta h_i > 0$  means that MIPAS was looking higher than indicated by the ETA.

Figure 2 gives an overview over typical features of the height dependence of  $\Delta h_i$  for a collection of several orbits, where each collection represents approximately one day (which is given in the headline of the panels). Only 13–14 values of  $\Delta h_i$  are shown in the respective panels, with lowest tangent altitudes in the range 16–18 km. This is because for the data presented only altitude levels where  $h_{\text{IMK},i}$  exists for at least 80% of each geolocation have been considered. Usually in the tropics there are cloud tops as high as 15 km. Tangent altitudes below these heights did not enter the LOS retrieval at IMK. So if there are more than 20% of geolocations contaminated with clouds, there will be no differences shown at all for the respective altitudes. The reason for this rather strict criterion is that, as we shall see in the subsequent sections of this paper, there are features like drifts in time and a dependence of the altitude differences from latitude, which might induce a bias due to sampling effects (clouds are not evenly distributed along orbit).

There is a change of the height profile of  $\Delta h_i$ -curves with time, where essentially two types can be found: Curves of the first type are like those presented in the two upper panels while examples of the second type can be found in the lower panels. The time

### Characterization of MIPAS elevation pointing

M. Kiefer et al.

Title Page

Abstract

Introduction

Conclusions

References

Tables

Figures

◀

▶

◀

▶

Back

Close

Full Screen / Esc

Printer-friendly Version

Interactive Discussion

when the curves change shape is around June of 2003. Before this date they have a slightly wavy appearance with local maxima typically at 27 and 38 km. Afterwards the upper local maximum at 38 km remains while the lower is shifted downwards to approximately 23 km. Though the main difference is that between the local minimum at 33 km and the maximum at 23 km there is an increase in  $\Delta h_i$  of around 300 m for the curves of second type while in those of first type it is below 200 m. Since no changes in the IMK retrieval scheme or set-up have been made, the change of the course of  $\Delta h_i$  with height must be attributed to changes of the engineering tangent altitude's characteristics.

Figure 3 shows, plotted over orbit number, rms-values of  $\Delta h_i$ -profiles, calculated for all geolocations of the respective orbits. Rms-values are about 200 m or less for orbit numbers from 3500 to 7300, with lowest values at around orbit 6000 (which corresponds to late April of 2003). Orbits greater than 7300 (late July of 2003) exhibit rms of around 200 m or more.

The course of  $\Delta h_i$  with height seems to be quite systematic and hence well characterized by the corresponding rms value. In the remainder of this paper we therefore use the average value at a geolocation

$$\Delta h = \frac{1}{N_{\text{tang}}} \sum_{i=\eta_{\text{low}}}^{17} \Delta h_i. \quad (1)$$

$\Delta h$  is considered to represent the average difference between the retrieved LOS tangent altitude and the engineering tangent altitude per geolocation to an accuracy given by the rms-value. Again  $\Delta h > 0$  for a geolocation means that on average MIPAS was looking higher than indicated by the engineering tangent altitudes.

### 3 Time dependence

Figure 4 shows the values of  $\Delta h$  in the course of a day for four different dates. Besides a periodic variation there is a jump at around 14:00–15:00 UTC discernible in the upper

## Characterization of MIPAS elevation pointing

M. Kiefer et al.

Title Page

Abstract

Introduction

Conclusions

References

Tables

Figures

◀

▶

◀

▶

Back

Close

Full Screen / Esc

Printer-friendly Version

Interactive Discussion

three panels of the figure. The cause of the jump is an update procedure for the on-board parameters of the platform's attitude, which is done twice a day at approximately 02:00 UTC and 14:00 UTC. In the vast majority of the data examined only the update procedure at 14:00 UTC shows an effect on  $\Delta h$ . The update at 02:00 UT is mostly perceptible as a slightly enhanced amplitude of the corresponding orbit variation. The size of the jump at 14 UTC of approximately 1–1.5 km, and the fact that the jump at 02:00 UTC is virtually absent, leads to a rough estimate for the trend of  $\Delta h$  over a day of 42–63 m/h or 70–107 m/orbit. In December 2003 there was a major update of the PSO which largely reduced the jump amplitude. The impact of the gain achieved is illustrated in the lowermost panel of Fig. 4.

There is a pronounced oscillation of  $\Delta h$  with a period which corresponds to one orbit, and an amplitude of approximately 1 km. This oscillation persists throughout the whole time span covered by the reprocessed MIPAS off-line data.

### 3.1 One orbit

In Fig. 5 there is shown  $\Delta h$  over one orbit. Clearly the extrema of the periodic variation are located at the poles. The course of  $\Delta h$  with latitude (lower panel of figure) can roughly be approximated by a line. Therefore a corresponding line fit was performed for all orbits considered henceforth. This fitted line is determined by an offset, i.e. the value at the equator, and a gradient, which is the slope of the line. These two quantities related to one orbit, offset and gradient, will be examined further.

Figure 6 shows histograms of offset values where only data before the major software update in December 2003 have been considered. In what follows two values characterizing the center of the histograms, namely arithmetic mean and median, will be given in the form mean/median. In the top left panel of Fig. 6 a histogram of all data is shown. The distribution is quite broad with its center at approximately  $-0.97/-1.02$  km. For the three other panels all data from a 1.5 h time window around 02:00 UTC and 14:00 UTC have been removed to avoid unwanted effects of the jumps discussed above. Additionally the data have been centered per day. This means that the daily av-

## Characterization of MIPAS elevation pointing

M. Kiefer et al.

Title Page

Abstract

Introduction

Conclusions

References

Tables

Figures

◀

▶

◀

▶

Back

Close

Full Screen / Esc

Printer-friendly Version

Interactive Discussion



erage value of the offset was subtracted from all single offset values of that day. Hence this procedure gives the variation of the offset around the daily mean value. In the top right panel the corresponding histogram is depicted, the centering on a daily basis of course shifts the distributions such that it is centered around zero. Clearly a double peaked distribution can be seen with the peaks approximately 350 m apart. If there was only a linear drift, as assumed in the preceding paragraph, one would expect a distribution with a rather flat top. The two lower panels separate the contributors of the two respective peaks. Data from 02:00–14:00 UTC (lower left panel) has a distribution which is centered at 0.17/0.16 km, while the distribution of data from 14:00–02:00 UTC is centered at –0.20/–0.18 km.

For the sake of completeness we give the corresponding results for data after the 12th of December 2003 (no corresponding plot shown): All data are centered at –0.55/–0.56 km, which is a little more than half of the average offset before that date. The data centered per day with removed data points in a 1.5 h time window around 02:00 UTC and 14:00 UTC are still distributed in a double peaked histogram that can be separated into two single peaked ones. Data from 02:00–14:00 UTC is centered at –0.03/–0.04 km, and data from 14:00–02:00 UTC at 0.04/0.05 km. Hence the peak separation is about a quarter of what it was before the 12 December. Obviously the software update largely improved the pointing of MIPAS with respect to the average offset.

As shown in Fig. 7 the gradient features a behaviour similar to the offset's. The double peaked structure can already be seen in the top left panel, which depicts the histogram of all gradient values of data before the major PSO software update. Arithmetic mean and median of this data set are 0.010/0.009 km°. After data from a 1.5 h time window around 02:00 UTC and 14:00 UTC have been removed, and the procedure of centering on a daily basis has been applied, the two peaks stand out even better separated (top right panel). Again the distribution of values clearly decomposes when split into the classes representing 02:00–14:00 UTC data and 14:00–02:00 UTC data (lower panels). The former is centered at –0.0010/–0.0011 km° while the latter's center

## Characterization of MIPAS elevation pointing

M. Kiefer et al.

Title Page

Abstract

Introduction

Conclusions

References

Tables

Figures

◀

▶

◀

▶

Back

Close

Full Screen / Esc

Printer-friendly Version

Interactive Discussion

is located at  $0.0012/0.0012 \text{ km}^\circ$ . Again an improvement of the data taken after the 12 December 2003 (not shown as plot) can be observed, however it is much smaller than the offset's: All data is centered at  $0.0096/0.0097 \text{ km}^\circ$ , data from 02:00–14:00 UTC at  $-0.0007/-0.0006 \text{ km}^\circ$ , and the 14:00–02:00 UTC data at  $0.0009/0.0009 \text{ km}^\circ$ .

5    3.2    Sucessive orbits

In Fig. 8 values of  $\Delta h$  for several subsequent orbits are shown, separated for ascending and descending parts of the respective orbits. Apart from offset, gradient, drift, and the dependence of the time slots 02:00–14:00 UTC and 14:00–02:00 UTC already discussed, there are two additional features standing out clearly. First a difference  
10    between the course of  $\Delta h$  between ascending and descending parts of orbits is discernible.  $\Delta h$  of descending orbit parts quite well follows a straight line, while in descending parts it exhibits a wavy appearance. This difference between ascending and descending parts of the orbits is a common feature of all data, while the specific form of the deviation from a straight line of the descending parts is not. The reason for the  
15    phenomenon is not clear yet and still under investigation.

Secondly there is an obvious persistence of fine structure in each case in curves of ascending and descending orbit parts. For the orbits shown in Fig. 8, in  $\Delta h$  of ascending orbit parts (upper panel), there is e.g. a marked W-shaped feature between latitudes  $-50^\circ$  and  $-25^\circ$ , a small positive peak at about  $0^\circ$ , and a small negative peak  
20    at about  $30^\circ$ . In descending orbits similar features as e.g. positive peaks at  $-30^\circ$  and  $-5^\circ$  and a negative bump around  $-40^\circ$  can be seen. This persistence of fine structure in  $\Delta h$  for subsequent orbits, bound to certain latitudes, again is a characteristic feature of the whole data set.

3.3    Correlation of LOS azimuth and  $\Delta h$

25    In the following we propose a possible reason for the persistent fine structure and the pole-to-pole gradient in  $\Delta h$ , based on the assumption of a roll angle of the satel-

Characterization of  
MIPAS elevation  
pointing

M. Kiefer et al.

Title Page	
Abstract	Introduction
Conclusions	References
Tables	Figures
◀◀	▶▶
◀	▶
Back	Close
Full Screen / Esc	
Printer-friendly Version	
Interactive Discussion	

lite/instrument, which is not accounted for in the data processing. As already described in Sect. 1 the LOS azimuth  $\alpha$  of MIPAS is changed periodically over the orbit to enhance the coverage of high latitudes. The adjustment of  $\alpha$  is not done in a continuous way but rather in steps. From geometric considerations it follows that a roll angle of the system, which is not accounted for, will firstly map the orbit periodic adjustment of  $\alpha$  into an orbit periodic variation of  $\Delta h$  and secondly map the azimuth steps into corresponding discontinuities in  $\Delta h$ . It has to be noted though, that a change of satellite pitch angle which had an appropriate orbit periodic part would create a very similar behaviour in  $\Delta h$  over latitude. Indeed there is an orbit periodic change in the pitch, but its magnitude is much smaller than the effect shown in Fig. 8. This will be discussed in more detail in Sect. 5.

Figure 9 gives an overview of the quantities involved. The left column of panels shows  $\Delta h$  (top) and LOS  $\alpha$  (center) against time, and a scatter plot of both quantities (bottom). In the right column quantities derived from  $\Delta h$  and  $\alpha$  are depicted.  $\Delta(\Delta h)$  is the difference of  $\Delta h$  of subsequent measurement geolocations/times.  $\Delta\alpha$  is defined in the same manner as the difference of the LOS azimuth of subsequent times.  $\Delta(\Delta h)$  (top) and  $\Delta\alpha$  (center) over time are shown while the bottom panel again contains the corresponding scatter plot.

$\Delta h$  plotted against time shows the orbit periodic feature as already discussed in Sect. 3.1. The LOS azimuth  $\alpha$  also shows a course periodic in time, with a period of one orbit. Maxima of  $\alpha$  of approximately  $110^\circ$  correspond to maxima in  $\Delta h$ , i.e. to measurements near the North Pole, while minima of  $\alpha$  of around  $75^\circ$  belong to the southern polar region.  $\Delta h$  and  $\alpha$  seem to be linearly correlated.  $\Delta(\Delta h)$  still exhibits some periodic feature but a strong noise component is visible. The course of  $\Delta\alpha$  over time shows, that the higher the corresponding latitudes are the smaller the changes in the commanded azimuth  $\alpha$  become. Around the Equator, which means around  $\alpha \approx 90^\circ$ , the changes are greatest. There seems to be a good linear correlation between  $\Delta\alpha$  and  $\Delta(\Delta h)$ , too.

The roll angle  $\rho$  can be estimated from a linearized model of the observation geom-

Characterization of  
MIPAS elevation  
pointing

M. Kiefer et al.

Title Page

Abstract

Introduction

Conclusions

References

Tables

Figures

◀

▶

◀

▶

Back

Close

Full Screen / Esc

Printer-friendly Version

Interactive Discussion

etry to be

$$\rho = \delta_{h,\alpha} \frac{1}{l_{\text{LOS}} \sin^2 \epsilon}, \quad (2)$$

where  $\delta_{h,\alpha}$  means either  $d\Delta h/d\alpha$  or  $d\Delta(\Delta h)/d\Delta\alpha$ ,  $\epsilon$  is the LOS elevation angle, and  $l_{\text{LOS}}$  means the distance between instrument and tangent point.

The two lowermost plots of Fig. 11 give values of  $\delta_{h,\alpha}$  of  $0.045 \text{ km}^\circ$ . With  $\epsilon \approx 116.5^\circ$  and  $l_{\text{LOS}} \approx 3200 \text{ km}$  the roll angle for orbits 2886–2887 can be estimated to approximately  $0.057^\circ$ . From the facts that near the North Pole  $\Delta h$  is greater than average and that there the azimuth is adjusted to have the LOS more towards the pole, we can infer that the rotation of the instrument/satellite system is counterclockwise with respect to the flight direction. In other words, there is a tilt to the left if one looks along the flight path.

### 3.4 Long term behaviour

To assess the long term trend of MIPAS pointing we again employ the quantities used in the preceding sections.

First offset and gradient which characterize the course of  $\Delta h$  over an entire orbit are examined. Again data from the time ranges 01:30–03:00 UTC and 13:30–15:00 UTC have been excluded. Figure 10 depicts the corresponding data. The upper panel shows offset values plotted against orbit number, where every diamond represents one orbit. The thick line connecting squares is the daily average. The scatter of the single orbit data is conspicuous, as already visible in Fig. 6. Now it is obvious that it has two main constituents: Firstly there is the scatter of data of one day which is the manifestation of the daily trend(s) in  $\Delta h$ , and consequently in the offset, as already discussed in Sect. 3.1. Secondly there is a multitude of trends of different time scales visible, some of which are separated by jumps. A major trend is visible between orbits 3500–8000 (begin of November 2002 through early September 2003). The daily mean of the offset in this time span changes from  $-1.3$  to  $-0.4 \text{ km}$  which corresponds to a

13086

## Characterization of MIPAS elevation pointing

M. Kiefer et al.

Title Page

Abstract

Introduction

Conclusions

References

Tables

Figures

◀

▶

◀

▶

Back

Close

Full Screen / Esc

Printer-friendly Version

Interactive Discussion

trend of 80 m/month. After a jump of offset values down to  $-1.6$  km around orbit 8100 there are two time ranges with quite constant values each, namely  $-1.6$  km at orbits 8100–8500 and  $-1.1$  km at orbits 8600–9200. Orbits greater than approximately 9300 (which corresponds to the date of the major software update) show significantly lower scatter in daily offset values as well as a relatively stable average value. This again is a manifestation of the quality gain achieved by the PSO software update. Gradient values (lower panel of Fig. 10) do not exhibit any clear indication of trend while the improvement in data scatter after 12 December 2003 is small. The details of this have already been discussed at Sect. 3.1.

The slopes of the fitted regression lines of azimuth angle and height offset are plotted over orbit number in Fig. 11. The upper panel shows the slopes of the pair  $\Delta h$  and  $\alpha$ , while in the lower slopes of the  $\Delta(\Delta h)$ - $\Delta\alpha$  correlation is drawn. Again only data which does not fall into the two time ranges of satellite attitude parameter updates (01:30–03:00 UTC and 13:30–15:00 UTC) have been considered. In principle, both slopes,  $d\Delta h/d\alpha$  and  $d\Delta(\Delta h)/d\Delta\alpha$  should have equal values.

As shown in Table 1 this essentially is true. However in  $d\Delta h/d\alpha$  there obviously is a slight difference between data sets restricted to 02:00–14:00 UTC and to 14:00–02:00 UTC.

As a general result we can state that, for the entire time examined here, there is evidence for a roll angle of the MIPAS measurement geometry of about  $54\pm6$  mdeg. With respect to the direction of flight the tilt is to the left.

#### 4 MIPAS operational pointing characterisation

As stated in Sect. 1.2, MIPAS pointing is particularly sensitive to the orientation of the satellite x- and y-axes (see Fig. 1). The instrument, therefore, can be exploited to determine accurate estimates of pitch and roll angles respectively. For this purpose, a dedicated measurement mode called “Line-Of-Sight Calibration Mode” was defined. In this mode the instrument is operated as a radiometer, i.e. the interferometer slides are

### Characterization of MIPAS elevation pointing

M. Kiefer et al.

Title Page

Abstract

Introduction

Conclusions

References

Tables

Figures

◀

▶

◀

▶

Back

Close

Full Screen / Esc

Printer-friendly Version

Interactive Discussion

driven to their end stops and the radiance emitted by bright infrared stars crossing the IFOV is measured.

The trajectory of the stars motion inside the EFOV is dependent upon the viewing direction. While looking in the rearward direction, due to the rotational motion of the satellite in its orbit, the stars have a trajectory approximately parallel to the nadir direction and therefore nearly perpendicular to the XY-plane. In order to acquire Line-Of-Sight (LOS) measurements in the rearward looking geometry, the IFOV is placed at a fixed elevation, near an approaching star and held up until the star has completely crossed the IFOV. The difference between the measured star crossing time and the expected crossing time is directly related to MIPAS mispointing caused by an error in the pitch angle.

When the instrument looks sideways, the star trajectories parallel to the nadir direction are seen as circular arcs within the EFOV. In this geometry, the IFOV is moved upwards at a pseudo-constant rate in elevation while scanning also in azimuth in order to keep the star azimuth-centred within the IFOV. Differences between actual and predicted star crossing times are again linked to the instrument pointing. Sideways measurements are particularly sensitive to mispointing due to the roll angle of the instrument.

The accuracy of the pointing measurements is strictly related to the accuracy achieved in the determination of the time at which a given star crosses the IFOV. In order to locate the star signal with a good accuracy, the signal-to-noise ratio of the measured radiance has to be increased by scanning repeatedly the same star several times and averaging the measured signals. Actually this operation is possible because MIPAS is capable of observing the same star for time intervals 40 s long (in the rearward direction). Therefore, since the nominal star crossing time is approximately 4 seconds, the same star can be observed up to ten times in succession.

During the measurements, the signal is acquired only from channels D1 and D2 (Endemann, 1999) and processed on-ground using detailed information concerning satellite orbit and platform attitude. Pointing errors are determined by fitting the mea-

Characterization of  
MIPAS elevation  
pointing

M. Kiefer et al.

Title Page

Abstract

Introduction

Conclusions

References

Tables

Figures

◀

▶

◀

▶

Back

Close

Full Screen / Esc

Printer-friendly Version

Interactive Discussion

surements with a six-parameters model that includes a bias and a sine variation of the pitch and roll error on the platform attitude as a function of the position along the orbit.

LOS measurements cover 2 subsequent orbits and about 60–80 star crossings are observed. The measurements are performed on a weekly basis and processed bi-weekly. This plan allows a proper monitoring of the pointing stability and guarantees the availability of pointing data in case of missing products (unavailability of products containing LOS measurements may be caused by instrument unavailability, failure in commands execution, data transfer problems, failure in data processing, etc.). The baseline for LOS calibration foresees that the absolute bias is compared with the last value disseminated in the ground segment, then a new LOS calibration Auxiliary Data File (ADF) is disseminated only if the absolute difference between the two biases is larger than 8 mdeg (corresponding to about 450 m in tangent height). The disseminated ADF contains pointing error knowledge to be used within L1b data processing to correct pointing during computation of the engineering tangent altitudes.

At the beginning of MIPAS mission, only LOS star measurements from detector D1 were analysed because this detector was less noisy than detector D2. However, starting from September 2003 the noise of channel D1 increased significantly (without impact on science data because this is a low frequency noise) and star signals were no longer visible. Detector D2 is currently used as backup, however, compared to the beginning of the mission, fewer stars are observed with good signal-to-noise ratio. To overcome this problem a new commanding scenario has been implemented in November 2004 in order to double the number of observable crossings per star and hence reduce the noise, but no evident improvements have been observed in the noise reduction. Due to the low signal-to-noise ratio of the LOS measurements, it is now hard to determine accurately the orbital variation of MIPAS mispointing. Therefore, the above mentioned fitting procedure is presently asked to extract only the bias of pointing errors.

In winter 2004, while investigations on the interferometer mirror drive anomaly were on-going and atmospheric measurements were not possible, the instrument has been exploited to perform an extensive set of LOS measurements. MIPAS LOS data have

**Characterization of  
MIPAS elevation  
pointing**

M. Kiefer et al.

Title Page

Abstract

Introduction

Conclusions

References

Tables

Figures

◀

▶

◀

▶

Back

Close

Full Screen / Esc

Printer-friendly Version

Interactive Discussion

been inter-compared with restituted attitude information from the Envisat star trackers, in preparation for future operational use of restituted attitude in off-line processing. Apart from a pitch bias of 24 mdeg, results from the MIPAS LOS campaign agree with star tracker information. Investigations are currently ongoing to find the cause of the observed pitch bias. Moreover, since November 2004, sideways measurements have been interrupted because the related processed data were not reliable. The prototype software for LOS processing is suspected to be the responsible for the degradation of the sideways LOS measurements, however investigations on this regard are still in progress.

In Fig. 12 we report the long term trend of MIPAS mispointing determined during the operational LOS characterization. The figure shows the absolute pointing bias as a function of the orbit number, in the time period from August 2002 to April 2005. Each point is obtained by averaging the values of the pointing error obtained from LOS calibration measurements collected during two full orbits. The conversion of the pointing error from angle (radians) to tangent altitude (km) was obtained simply multiplying the angles by 3200 km, the average distance between the satellite and the tangent point of typical limb measurements. The pronounced variation of the pointing bias at the beginning of the mission was not related to the MIPAS instrument itself, but to an anomalous behaviour of the attitude of the entire ENVISAT satellite. This anomaly was the result of the erroneous response of the PSO software to the orbit control information. In fact, after the update of the PSO software, implemented on 12 December 2003 (orbit 9321), the amplitude of the variations of the pointing bias was drastically reduced.

## 5 Results of other instruments or characterization methods

### 5.1 MIPAS

There is an ESA technical note on the ENVISAT Restituted Pitch Assessment (Saavedra et al., 2005) which deals with dedicated LOS calibration measurements of the

## Characterization of MIPAS elevation pointing

M. Kiefer et al.

Title Page

Abstract

Introduction

Conclusions

References

Tables

Figures

◀

▶

◀

▶

Back

Close

Full Screen / Esc

Printer-friendly Version

Interactive Discussion



limb-viewing instruments onboard ENVISAT to obtain a characterization of the platform's pitch. Several results presented in the report can be directly compared to those of Sects. 2–3, although the data of Saavedra et al. (2005) is based on special MIPAS LOS calibration orbits (see preceding section).

The results with respect to the long term behaviour are discussed above in Sect. 4. As a further result there is found an indication for an orbit periodic pitch variation with an amplitude of about 3–4 mdeg. The pitch variation would have an orbit periodic effect in  $\Delta h$  of 170–220 m amplitude, i.e. much less than what is presented in Sect. 3.3. No roll angle effects are considered by Saavedra et al. (2005).

At the 8th meeting of the MIPAS quality working group in September 2005, Anu Dudhia of Oxford University has reported about retrieval results of MIPAS observations in the aircraft emission mode. This is a special mode where MIPAS is looking sideways, the respective measurements have been taken with azimuth angles of  $\alpha=160^\circ$  and  $\alpha=190^\circ$ . Anu Dudhia stated that the engineering altitudes reported in the L1b data are about 5 km too low. This is in rough agreement with our results, both in sign and magnitude, since for  $\alpha=180^\circ$  we get  $\Delta h=3$  km for a roll angle of 54 mdeg.

## 5.2 GOMOS

Saavedra et al. (2005) show analyses of GOMOS mispointing which hint to a orbit-periodic variation of amplitude in the order of some mdeg. This in accordance with MIPAS results, see Sect. 5.1.

Further there might be an indication of an uncorrected roll angle. This can be inferred from their Fig. 2-1, where GOMOS elevation mispointing is plotted over azimuth angle. The elevation mispointing clearly decreases from around zero at zero azimuth to  $-20$  mdeg at  $80^\circ$  azimuth. Extrapolation to  $90^\circ$  would give a value of about  $-25$  mdeg which corresponds to a tangent altitude offset of 1.4 km. It has to be noted though, that the course of the dependence of elevation mispointing on azimuth angle does not fit to what would be expected from a roll angle problem. Further investigations on this problem are necessary.

### Characterization of MIPAS elevation pointing

M. Kiefer et al.

Title Page

Abstract

Introduction

Conclusions

References

Tables

Figures

◀

▶

◀

▶

Back

Close

Full Screen / Esc

Printer-friendly Version

Interactive Discussion

A spatial and temporal characterization of SCIAMACHY limb pointing errors is presented by [von Savigny et al. \(2005\)](#). A specific feature of the height profile of O<sub>3</sub> radiation in the UV is employed to gain information about the true tangent altitudes.

Since the method relies on horizontally homogeneous atmospheres, the results are valid only in a latitude band of  $\pm 20^\circ$  around the equator. The differences of engineering tangent altitudes and retrieved tangent altitudes are averaged over orbits only for these equatorial geolocations. The resulting quantity is called offset. The time span covered is July 2002 through February 2005 with a data gap of 3.5 months in the summer of 2003.

The main results are, that there is a mean offset, a drift, a seasonal variation, and an occurrence of two daily jumps. The characteristics of the respective phenomena are different before and after the major update of the PSO-algorithm software on 12 December 2003. While the drift, the amplitude of the seasonal variation, and the magnitude of the 14:00 UTC jump are lower after the software update, the average offset increases as well as the magnitude of the 02:00 UTC jump.

To compare the offset results presented in [von Savigny et al. \(2005\)](#) with  $\Delta h$ , it is important to note that SCIAMACHY is looking forward with respect to the MIPAS flight path. The definition of the height difference as above gives a reversal of sign compared to our definition. The impact of the two combined facts is that the SCIAMACHY results should be directly comparable to the data presented here, given that both instrument's main source for mispointing is the attitude error of the platform.

The constant offset component seen with SCIAMACHY is 500 m before and 1 km after 12 December 2003. The sign of the change seems to be compatible with our results while, due to the drift and jump features discussed in Sect. 3.4 there is no meaningful average value of the data before the date of the PSO software update. In our data we do not find an indication of a seasonal variation. As already discussed we find a trend of roughly 80 m/month between orbits 3500 and 8000. This corresponds at

**Characterization of  
MIPAS elevation  
pointing**

M. Kiefer et al.

Title Page

Abstract

Introduction

Conclusions

References

Tables

Figures

◀

▶

◀

▶

Back

Close

Full Screen / Esc

Printer-friendly Version

Interactive Discussion

least in sign to 30 m/month reported for the SCIAMACHY data of the time before 12th of December 2003. As von Savigny et al. (2005) we see that the jump at 14:00 UTC nearly vanishes after this date, however our data basis is not sufficient to either confirm or deny their statement that the 02:00 UTC jump has become worse.

## 6 Summary and conclusions

We have presented a characterization of MIPAS pointing elevation for two quantities which, on different stages of the data processing, represent the knowledge of the tangent altitudes. The results of the operation LOS calibration measurements based on star tracking are discussed in Sect. 4, while in Sects. 2–3 results of a LOS retrieval are presented.

We have examined several aspects of the mispointing which is gained as retrieval result from the L1b data. First there is a height dependence of the differences between retrieved tangent altitudes and engineering tangent altitudes. However this height dependence is very systematic and quite stable over a time span of almost two years. Further it is compatible with the estimates of systematic errors which are to be expected for the LOS retrieval (von Clarmann et al., 2003). We take the well defined shape of the height dependence as justification to regard one single value, namely the average of the differences, as a representative quantity for the mispointing at a given geolocation.

Before 12 December 2003 jumps, which occur twice a day, are a regular feature of time series of the mispointing. The first jump at around 02:00 UTC usually is small while the second one at around 14:00 UTC is conspicuous and can reach values of 2 km. Most quantities which characterize the mispointing show a clear dependence on whether they are calculated in the interval 02:00–14:00 UTC or 14:00–02:00 UTC. The cause for the jumps has been identified by ESA to be the erroneous response of the PSO software to the orbit control information uploaded twice a day. After an update of the PSO software on 12 December 2003 at least the size of the jump at 14:00 UTC is

### Characterization of MIPAS elevation pointing

M. Kiefer et al.

Title Page

Abstract

Introduction

Conclusions

References

Tables

Figures

◀

▶

◀

▶

Back

Close

Full Screen / Esc

Printer-friendly Version

Interactive Discussion

much reduced. Our finding is confirmed by von Savigny et al. (2005), who additionally state that the size of the 02:00 UTC jump has increased after the respective software update.

The result that there is a strong dependence on latitude of the mispointing, together with the observation that there are common small scale features in successive orbits, leads us to suggest that there is a roll angle in the platform/instrument system which currently is not accounted for. A roll angle of  $54 \pm 6$  mdeg, corresponding to a tilt to the left, referring to the flight direction, would explain a bigger part of the latitudinal behaviour of the mispointing. An explanation of the latitude dependence based on an orbit periodic pitch variation alone can be ruled out, since the operational LOS calibration for MIPAS and GOMOS gives values for this effect, which are an order of magnitude below what we actually find. However the particular course of the mispointing on descending orbit parts remains to be explained.

For examination of the longterm behaviour we took the retrieval results as well as dedicated LOS calibration measurements. Although the results can not be compared directly, because the LOS calibration measurements give absolute pointing deviations, while the engineering altitudes already contain corrections for mispointing gained by the LOS calibration, it is interesting to see, that some features are well visible in both data sets. This is depicted in Fig. 13 which shows data from the jump in mispointing around orbit 8100 until the end of March 2004 (major MIPAS failure) and includes the date of the PSO software update on 12 December 2003. Apart from the fact that the absolute mispointing has shifted up by 1.1 km the overall runs of the two data sets do match quite well.

Finally it has to be noted that it is impossible to give a general and simple correction scheme for the engineering tangent altitudes. Although some of the systematic deviations could be reduced, e.g. the impact of the roll angle, many others, less well defined ones, can not.

From this it follows, that comparison and validation work which uses MIPAS data should be based only on the tangent pressure values delivered with the ESA L2 prod-

Characterization of  
MIPAS elevation  
pointing

M. Kiefer et al.

Title Page

Abstract

Introduction

Conclusions

References

Tables

Figures

◀

▶

◀

▶

Back

Close

Full Screen / Esc

Printer-friendly Version

Interactive Discussion

ucts, and avoid tangent altitudes as reference. To avoid confusion: L2 data products generated with the IMK processor are not affected by the detected pointing fluctuations because the retrieved pointing information is used.

*Acknowledgements.* F. Niro (Serco), and R. Koopman (ESA/ESRIN) have provided data and documents.

References

Bertaux, J. L., Hauchecorne, A., Dalaudier, F., Cot, C., Kyrölä, E., Fussen, D., Tamminen, J., Leppelmeier, G. W., Sofieva, V., Hassinen, S., Fanton d’Andon, O., Barrot, G., Mangin, A., Théodore, B., Guirlet, M., Korablev, O., Snoeij, P., Koopman, R., and Fraise, R.: First results on GOMOS/ENVISAT, *Adv. Space Res.*, 33, 1029–1035, 2004. [13077](#)

Bovensmann, H., Burrows, J. P., Buchwitz, M., Frerick, J., Noël, S., Rozanov, V. V., Chance, K. V., and Goede, A. P. H.: SCIAMACHY: Mission objectives and measurement modes, *J. Atmos. Sci.*, 56, 127–150, 1999. [13077](#)

Endemann, M.: MIPAS Instrument Concept and Performance, in *Proceedings of European Symposium on Atmospheric Measurements from Space*, Noordwijk, Netherlands, 18–22 January, vol. WPP-161, pp. 29–43, European Space Agency, ESTEC, Noordwijk, The Netherlands, 1999. [13088](#)

Fischer, H. and Oelhaf, H.: Remote sensing of vertical profiles of atmospheric trace constituents with MIPAS limb-emission spectrometers, *Appl. Opt.*, 35, 2787–2796, 1996. [13077](#)

Kyrölä, E., Tamminen, J., Leppelmeier, G. W., Sofieva, V., Hassinen, S., Bertaux, J. L., Hauchecorne, A., Dalaudier, F., Cot, C., Korablev, O., Fanton d’Andon, O., Barrot, G., Mangin, A., Théodore, B., Guirlet, M., Etanchaud, F., Snoeij, P., Koopman, R., Saavedra, L., Fraise, R., Fussen, D., and Vanhellemont, F.: GOMOS on Envisat: an overview, *Adv. Space Res.*, 33, 1020–1028, 2004. [13077](#)

Ridolfi, M., Carli, B., Carlotti, M., von Clarmann, T., Dinelli, B., Dudhia, A., Flaud, J.-M., Höpfner, M., Morris, P. E., Raspollini, P., Stiller, G., and Wells, R. J.: Optimized Forward and Retrieval Scheme for MIPAS Near-Real-Time Data Processing, *Appl. Opt.*, 39, 1323–1340, 2000. [13077](#), [13079](#)

Saavedra, L., Mantovani, R., and Dehn, A.: ENVISAT Restituted Pitch Assessment, Technical Note ENVI-SPPA-EOPG-TN-05-0011, ESA, 2005. [13090](#), [13091](#)

Characterization of MIPAS elevation pointing

M. Kiefer et al.

Title Page	
Abstract	Introduction
Conclusions	References
Tables	Figures
◀	▶
◀	▶
Back	Close
Full Screen / Esc	
Printer-friendly Version	
Interactive Discussion	

- von Clarmann, T., Glatthor, N., Grabowski, U., Höpfner, M., Kellmann, S., Kiefer, M., Linden, A., Mengistu Tsidu, G., Milz, M., Steck, T., Stiller, G. P., Wang, D. Y., Fischer, H., Funke, B., Gil-López, S., and López-Puertas, M.: Retrieval of temperature and tangent altitude pointing from limb emission spectra recorded from space by the Michelson Interferometer for Passive Atmospheric Sounding (MIPAS), J. Geophys. Res., 108, 2003. [13077](#), [13078](#), [13093](#)
- 5 von Savigny, C., Kaiser, J. W., Bovensmann, H., Burrows, J. P., McDonald, I. S., and Leblanc, T.: Spatial and temporal characterization of SCIAMACHY limb pointing errors during the first three years of the mission, Atmos. Chem. Phys., 5, 2593–2602, 2005, <http://www.atmos-chem-phys.net/5/2593/2005/>. [13092](#), [13093](#), [13094](#)

**Characterization of  
MIPAS elevation  
pointing**

M. Kiefer et al.

Title Page

Abstract

Introduction

Conclusions

References

Tables

Figures

I◀

▶I

◀

▶

Back

Close

Full Screen / Esc

Printer-friendly Version

Interactive Discussion

**Characterization of  
MIPAS elevation  
pointing**

M. Kiefer et al.

**Table 1.** Statistics of slopes of fitted lines.

Statistics of $d\Delta h/d\alpha$			
time range	mean [km/°]	std. dev. [km/°]	median [km/°]
02:00–14:00 UTC	0.036	0.005	0.036
14:00–02:00 UTC	0.044	0.004	0.044
00:00–24:00 UTC	0.040	0.004	0.040
Statistics of $d\Delta(\Delta h)/d\Delta\alpha$			
time range	mean [km/°]	std. dev. [km/°]	median [km/°]
02:00–14:00 UTC	0.042	0.004	0.042
14:00–02:00 UTC	0.042	0.007	0.043
00:00–24:00 UTC	0.042	0.005	0.043

Title Page

Abstract

Introduction

Conclusions

References

Tables

Figures

◀

▶

◀

▶

Back

Close

Full Screen / Esc

Printer-friendly Version

Interactive Discussion

## Characterization of MIPAS elevation pointing

M. Kiefer et al.

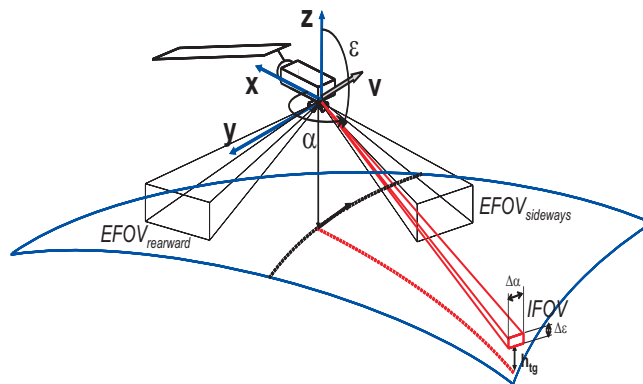


**Fig. 1.** Setup of MIPAS on ENVISAT. The flight direction of the platform is given by  $V$  and the satellite-fixed coordinate system by  $X$ ,  $Y$ , and  $Z$ . The Line-Of-Sight azimuth and elevation are  $\alpha$  and  $\epsilon$  respectively.

[Title Page](#)
[Abstract](#)
[Introduction](#)
[Conclusions](#)
[References](#)
[Tables](#)
[Figures](#)
[◀](#)
[▶](#)
[◀](#)
[▶](#)
[Back](#)
[Close](#)
[Full Screen / Esc](#)
[Printer-friendly Version](#)
[Interactive Discussion](#)



**Characterization of  
MIPAS elevation  
pointing**

M. Kiefer et al.

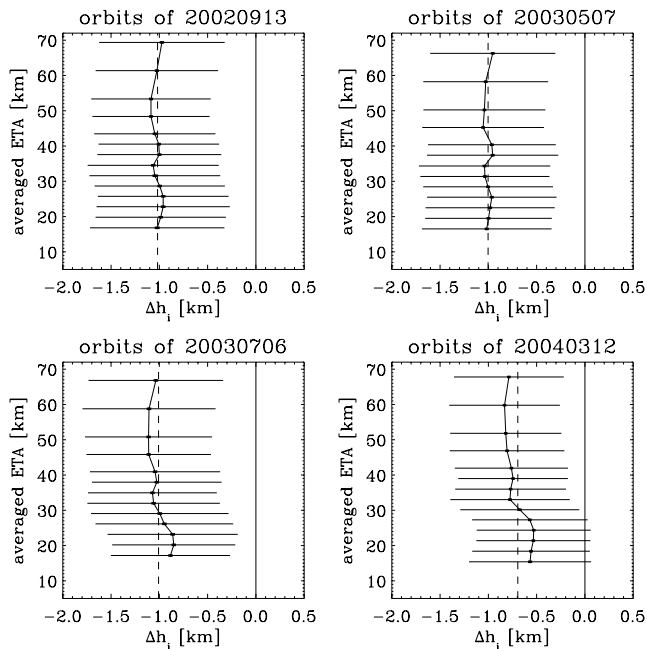


**Fig. 2.** Altitude dependence of  $\Delta h_i$  for all orbits of the four days indicated in the panel's headline. Broken lines indicate the average value, thin horizontal lines indicate the standard deviation, and thick horizontal lines give the standard deviation divided by the square root of the number of contributing values. Only heights where at least 80% of data of all corresponding geolocations were available have been considered to minimize bias by sampling effects.

Title Page

Abstract

Introduction

Conclusions

References

Tables

Figures

◀

▶

◀

▶

Back

Close

Full Screen / Esc

Printer-friendly Version

Interactive Discussion

## Characterization of MIPAS elevation pointing

M. Kiefer et al.

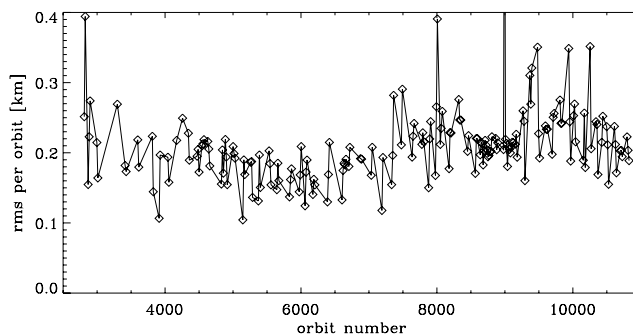


**Fig. 3.** Rms-values of  $\Delta h_i$ -profiles, collected for all geolocations of one orbit each, plotted against orbit number.

[Title Page](#)[Abstract](#)[Introduction](#)[Conclusions](#)[References](#)[Tables](#)[Figures](#)[◀](#)[▶](#)[◀](#)[▶](#)[Back](#)[Close](#)[Full Screen / Esc](#)[Printer-friendly Version](#)[Interactive Discussion](#)

**Characterization of  
MIPAS elevation  
pointing**

M. Kiefer et al.

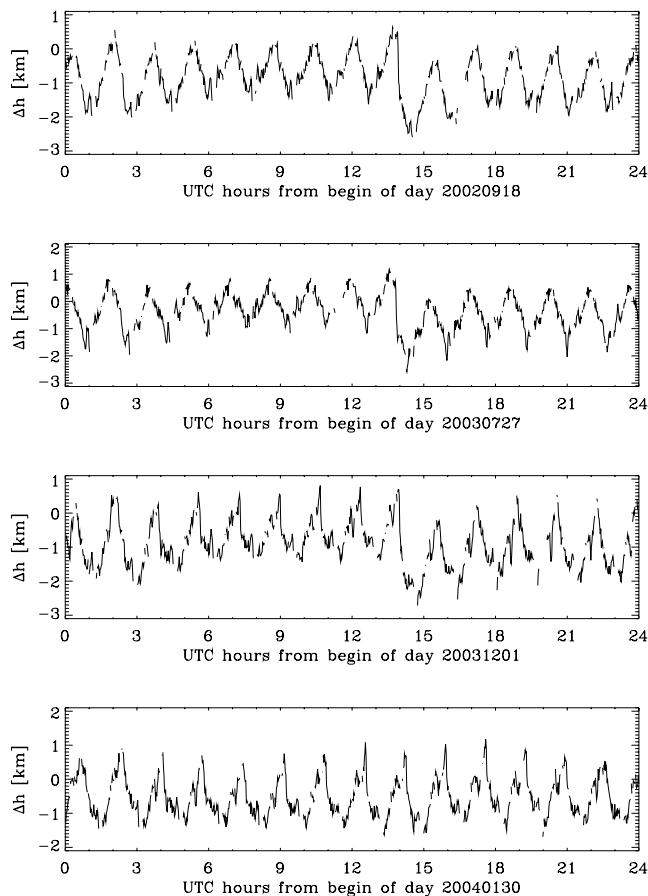


**Fig. 4.**  $\Delta h$  in the course of a day for four different dates. The upper three panels represent three dates before the major update of the PSO-algorithm software on 12 December 2003, while the lowest panel shows a date two weeks after the update.

[Title Page](#)[Abstract](#)[Introduction](#)[Conclusions](#)[References](#)[Tables](#)[Figures](#)[◀](#)[▶](#)[◀](#)[▶](#)[Back](#)[Close](#)[Full Screen / Esc](#)[Printer-friendly Version](#)[Interactive Discussion](#)

**Characterization of  
MIPAS elevation  
pointing**

M. Kiefer et al.

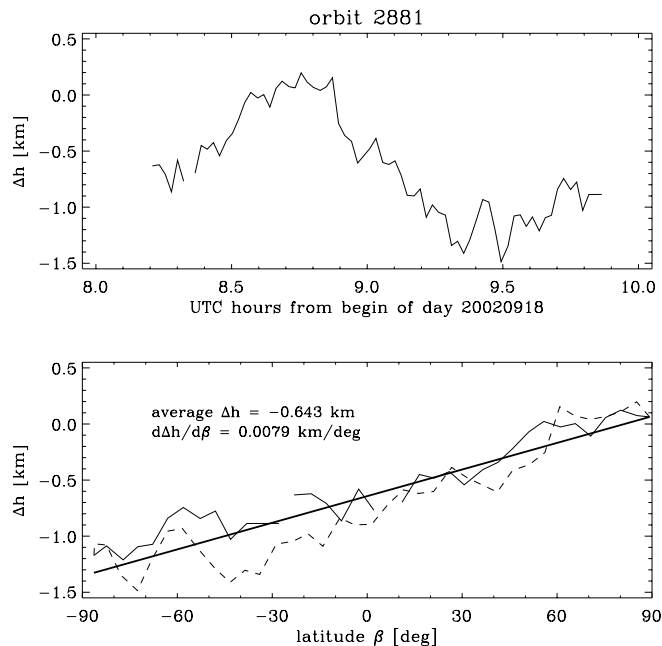


**Fig. 5.**  $\Delta h$  of orbit 2881 plotted against UTC (upper panel) and against geographical latitude  $\beta$  (lower panel). In the lower panel the thin solid and broken lines represent values of  $\Delta h$  for the ascending and descending part of the orbit, respectively. The thick solid line is the line fitted to the data. The two parameters determining the line are given in the plot frame as average  $\Delta h$ , i.e. the value at the equator, and  $d\Delta h/d\beta$ , i.e. the slope or gradient.

Title Page

Abstract

Introduction

Conclusions

References

Tables

Figures

◀

▶

◀

▶

Back

Close

Full Screen / Esc

Printer-friendly Version

Interactive Discussion

**Characterization of  
MIPAS elevation  
pointing**

M. Kiefer et al.

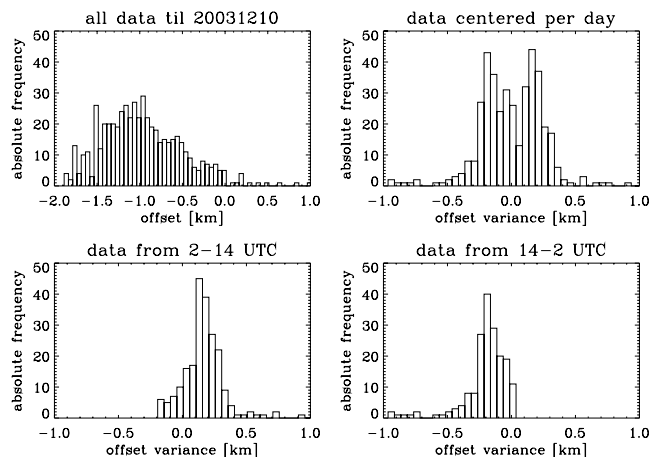


**Fig. 6.** Histograms of the offset of  $\Delta h$ . Top left panel: All data before 10 December 2003 (i.e. before the major software update). Top right panel: Data centered on a daily basis (mean value becomes zero). Lower two panels show the data centered per day for offset values of orbits between 02:00 UTC and 14:00 UTC (left) and between 14:00 UTC and 02:00 UTC (right). Binning is equal in all panels.

Title Page

Abstract

Introduction

Conclusions

References

Tables

Figures

◀

▶

◀

▶

Back

Close

Full Screen / Esc

Printer-friendly Version

Interactive Discussion

**Characterization of  
MIPAS elevation  
pointing**

M. Kiefer et al.

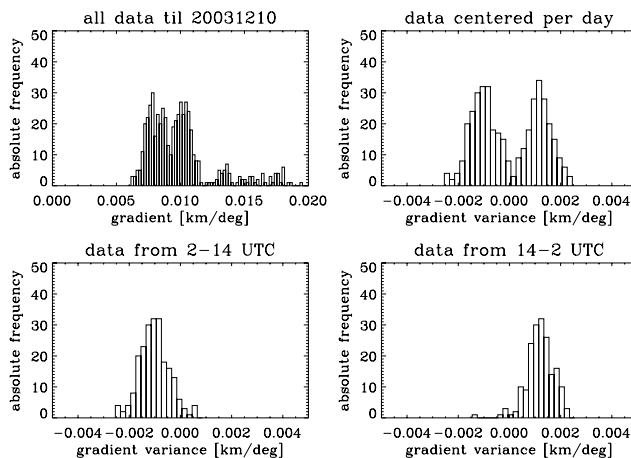


**Fig. 7.** Histograms of the gradient of  $\Delta h$  with respect to latitude. Type of data restrictions as in Fig. 6. Binning is equal in all panels.

[Title Page](#)[Abstract](#)[Introduction](#)[Conclusions](#)[References](#)[Tables](#)[Figures](#)[◀](#)[▶](#)[◀](#)[▶](#)[Back](#)[Close](#)[Full Screen / Esc](#)[Printer-friendly Version](#)[Interactive Discussion](#)

**Characterization of  
MIPAS elevation  
pointing**

M. Kiefer et al.

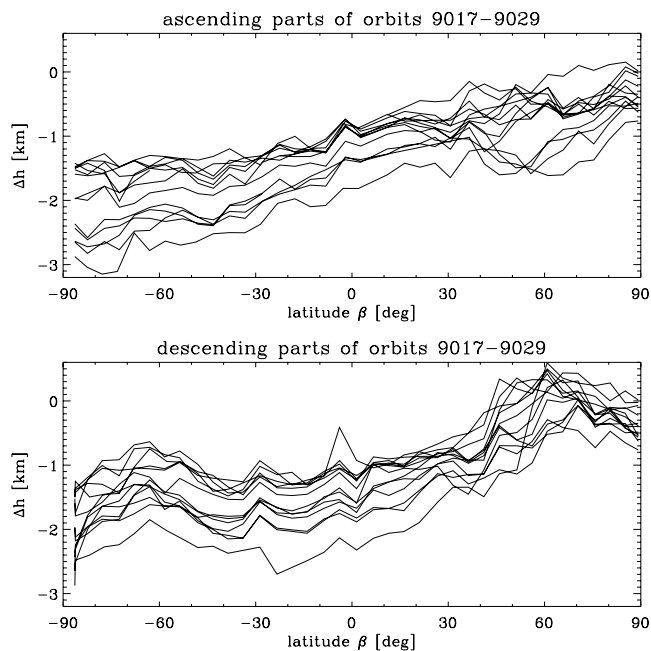


**Fig. 8.**  $\Delta h$  of several orbits, separated into ascending (upper panel) and descending (lower panel) parts of the orbits are plotted against geographical latitude.

[Title Page](#)[Abstract](#)[Introduction](#)[Conclusions](#)[References](#)[Tables](#)[Figures](#)[◀](#)[▶](#)[◀](#)[▶](#)[Back](#)[Close](#)[Full Screen / Esc](#)[Printer-friendly Version](#)[Interactive Discussion](#)

# Characterization of MIPAS elevation pointing

M. Kiefer et al.

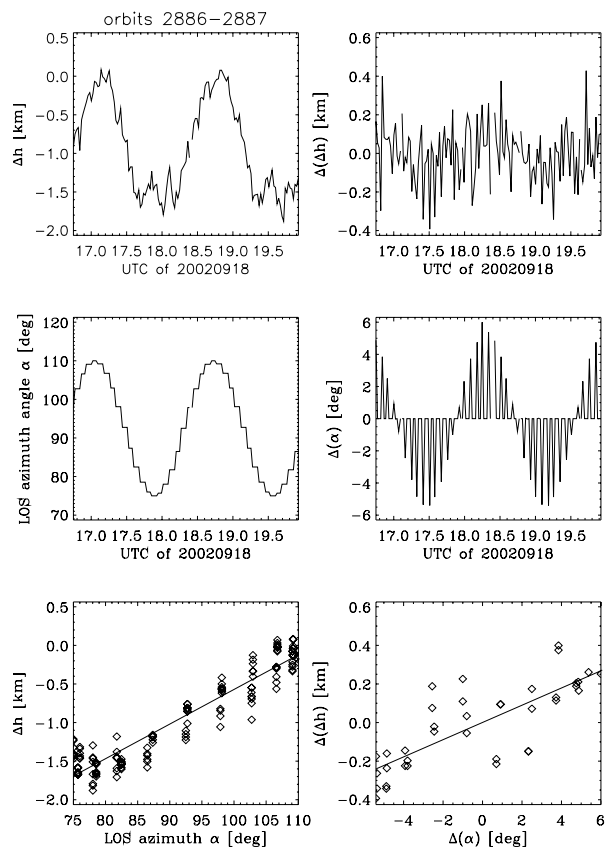


**Fig. 9.** Correlation of  $\Delta h$  and azimuth  $\alpha$ . Left column shows  $\Delta h$  and  $\alpha$  against time (top and middle panel, respectively), and the corresponding scatter plot (bottom). Right column has  $\Delta(\Delta h)$  and  $\Delta\alpha$  against time and the scatter plot of both. Both scatter plots have a fitted straight line overplotted. The definition of the quantities is given in the text.

[Title Page](#)
[Abstract](#)
[Introduction](#)
[Conclusions](#)
[References](#)
[Tables](#)
[Figures](#)
[◀](#)
[▶](#)
[◀](#)
[▶](#)
[Back](#)
[Close](#)
[Full Screen / Esc](#)
[Printer-friendly Version](#)
[Interactive Discussion](#)



## Characterization of MIPAS elevation pointing

M. Kiefer et al.

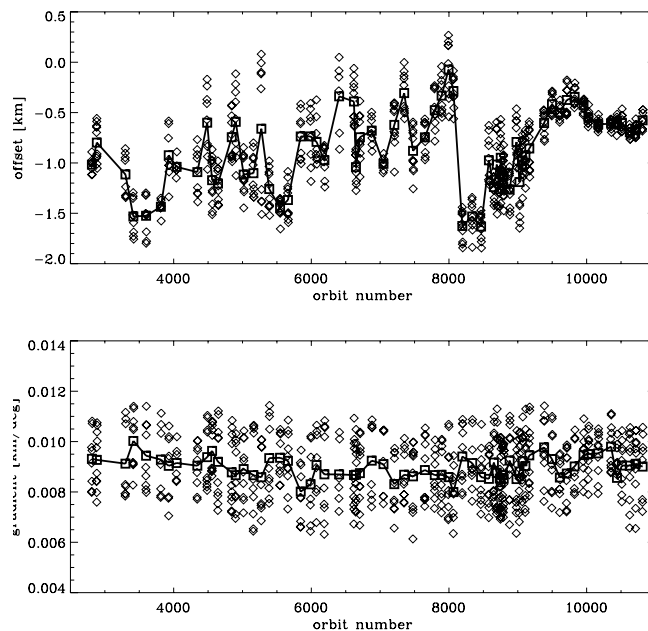


**Fig. 10.** Offset (top) and gradient (lower panel) drawn over orbit number. Only days with at least 500 processed geolocations have been taken. Each diamond represents a value of a single orbit. The daily average is marked by thick lines connecting squares.

[Title Page](#)[Abstract](#)[Introduction](#)[Conclusions](#)[References](#)[Tables](#)[Figures](#)[◀](#)[▶](#)[◀](#)[▶](#)[Back](#)[Close](#)[Full Screen / Esc](#)[Printer-friendly Version](#)[Interactive Discussion](#)

**Characterization of  
MIPAS elevation  
pointing**

M. Kiefer et al.

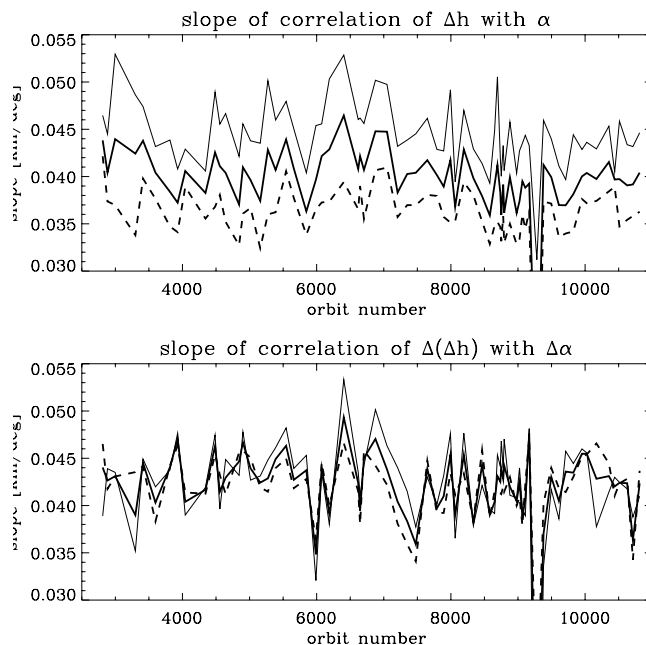


**Fig. 11.** Slope of the lines fitted to  $\Delta h$  and  $\alpha$  (upper panel) and to  $\Delta(\Delta h)$  and  $\Delta\alpha$  (lower panel) plotted over orbit number. Thick solid lines represent the slopes for all data. Thin solid lines give data of the time intervals 14:00–02:00 UTC while thick broken lines mark data of time interval 02:00–14:00 UTC.

[Title Page](#)[Abstract](#)[Introduction](#)[Conclusions](#)[References](#)[Tables](#)[Figures](#)[◀](#)[▶](#)[◀](#)[▶](#)[Back](#)[Close](#)[Full Screen / Esc](#)[Printer-friendly Version](#)[Interactive Discussion](#)

## Characterization of MIPAS elevation pointing

M. Kiefer et al.

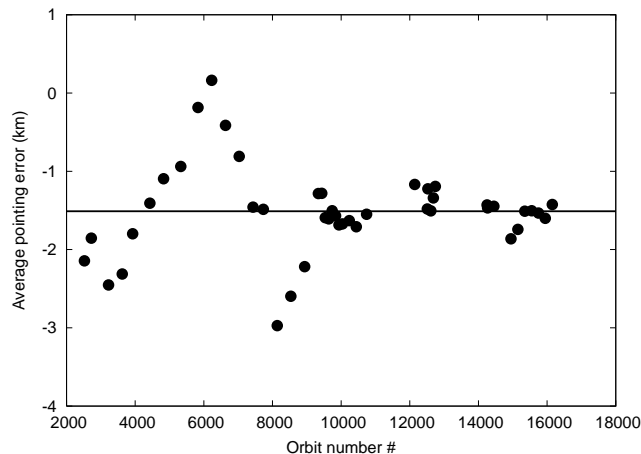


**Fig. 12.** MIPAS pointing bias as a function of the orbit number, from August 2002 to April 2005. The horizontal solid line represents the average value of the pointing bias.

[Title Page](#)[Abstract](#)[Introduction](#)[Conclusions](#)[References](#)[Tables](#)[Figures](#)[◀](#)[▶](#)[◀](#)[▶](#)[Back](#)[Close](#)[Full Screen / Esc](#)[Printer-friendly Version](#)[Interactive Discussion](#)

## Characterization of MIPAS elevation pointing

M. Kiefer et al.

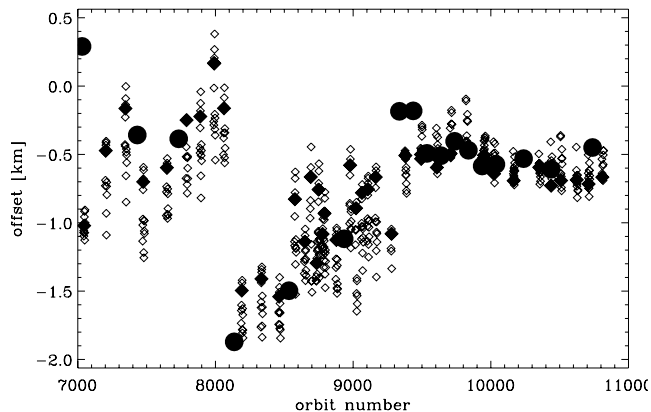


**Fig. 13.** Comparison of quantities characterizing the mispointing: Big filled circles are the same data as presented in Fig. 12, but shifted 1.1 km up, while diamonds are the data as shown in the upper panel of Fig. 10. Filled diamonds correspond to orbits which start around 07:00 UTC, the approximate start time of the LOS calibration orbits.

[Title Page](#)[Abstract](#)[Introduction](#)[Conclusions](#)[References](#)[Tables](#)[Figures](#)[◀](#)[▶](#)[◀](#)[▶](#)[Back](#)[Close](#)[Full Screen / Esc](#)[Printer-friendly Version](#)[Interactive Discussion](#)